Optically-programmable nonlinear photonic component for dielectric-loaded plasmonic circuitry

Alexey V. Krasavin,[1,4,*] **Sukanya Randhawa,**[2,4] **Jean-Sebastien Bouillard,**[1,4] **Jan Renger,**[2] **Romain Quidant,**[2,3] **and Anatoly V. Zayats**[1]

[1]*Department of Physics, King's College London, Strand, London WC2R 2LS, UK*
[2]*ICFO - Institut de Ciències Fotòniques, 08860 Castelldefels (Barcelona), Spain*
[3]*ICREA-Institució Catalana de Recerca i Estudis Avançats, 08010 Barcelona, Spain*
[4]*These authors contributed equally to this work.*
**alexey.krasavin@kcl.ac.uk*

Abstract: We demonstrate both experimentally and numerically a compact and efficient, optically tuneable plasmonic component utilizing a surface plasmon polariton ring resonator with nonlinearity based on trans-cis isomerization in a polymer material. We observe more than 3-fold change between high and low transmission states of the device at milliwatt control powers ($\sim$100 W/cm^2 by intensity), with the performance limited by switching speed of the material. Such plasmonic components can be employed in optically programmable and reconfigurable integrated photonic circuitry.

© 2011 Optical Society of America

OCIS codes: (190.4390) Nonlinear optics, integrated optics; (130.1750) Components; (250.5403) Plasmonics.

References and links

1. S. I. Bozhevolnyi, *Plasmonic Nanowaveguides and Cirquits* (Pan Stanford Publishing, 2009).
2. D. Pacifici, H. J. Lezec, and H. A. Atwater, "All-optical modulation by plasmonic excitation of CdSe quantum dots," Nat. Photonics **1,** 402–406 (2008).
3. G. A. Wurtz, R. Pollard, W. Hendren, G. P. Wiederrecht, D. J. Gosztola, V. A. Podolskiy, and A. V. Zayats, "Designed ultrafast optical nonlinearity in a plasmonic nanorod metamaterial enhanced by nonlocality," Nat. Nanotechnol. **6,** 107–111 (2011).
4. K. F. MacDonald, Z. L. Sámson, M. I. Stockman, and N. I. Zheludev, "Ultrafast active plasmonics," Nat. Photonics **3,** 55–58 (2009).
5. R. A. Pala, K. T. Shimizu, N. A. Melosh, and M. L. Brongersma, "A nonvolatile plasmonic switch employing photochromic molecules," Nano Lett. **8,** 1506–1510 (2008).
6. P. R. Evans, G. A. Wurtz, W. R. Hendren, R. Atkinson, W. Dickson, A. V. Zayats, and R. J. Pollard, "Electrically switchable nonreciprocal transmission of plasmonic nanorods with liquid crystal," Appl. Phys. Lett. **91,** 043101 (2007).
7. J. Gosciniak, S. I. Bozhevolnyi, T. B. Andersen, V. S. Volkov, J. Kjelstrup-Hansen, L. Markey, and A. Dereux, "Thermo-optic control of dielectric-loaded plasmonic waveguide components," Opt. Express **18,** 1207–1216 (2010), `http://www.opticsinfobase.org/oe/abstract.cfm?URI=oe-18-2-1207`.
8. T. Holmgaard, Z. Chen, S. I. Bozhevolnyi, L. Markey, A. Dereux, A. V. Krasavin, and A. V. Zayats, "Bend- and splitting loss of dielectric-loaded surface plasmon-polariton waveguides," Opt. Express **16,** 13585–13592 (2008), `http://www.opticsinfobase.org/oe/abstract.cfm?URI=oe-16-18-13585`.
9. B. Steinberger, A. Hohenau, H. Ditlbacher, F. R. Aussenegg, A. Leitner, and J. R. Krenn, "Dielectric stripes on gold as surface plasmon waveguides: Bends and directional couplers," Appl. Phys. Lett. **91,** 081111 (2007).

#153017 - $15.00 USD Received 16 Aug 2011; revised 1 Nov 2011; accepted 11 Nov 2011; published 23 Nov 2011
(C) 2011 OSA

10. A. V. Krasavin and A. V. Zayats, "Three-dimensional numerical modeling of photonic integration with dielectric-loaded SPP waveguides," Phys. Rev. B **78,** 045425 (2008).
11. O. Tsilipakos, T. V. Yioultsis, and E. E. Kriezis, "Theoretical analysis of thermally tunable microring resonator filters made of dielectric-loaded plasmonic waveguides," J. Appl. Phys. **106,** 093109 (2009).
12. T. Holmgaard, Z. Chen, S. I. Bozhevolnyi, L. Markey, A. Dereux, A. V. Krasavin, and A. V. Zayats, "Wavelength selection by dielectric-loaded plasmonic components," Appl. Phys. Lett. **94,** 051111 (2009).
13. S. Randhawa, A. V. Krasavin, T. Holmgaard, J. Renger, S. I. Bozhevolnyi, A. V. Zayats, and R. Quidant, "Experimental demonstration of dielectric-loaded plasmonic waveguide disk resonators at telecom wavelengths," Appl. Phys. Lett. **98,** 161102 (2011).
14. A. V. Krasavin and A. V. Zayats, "Electro-optic switching element for dielectric-loaded surface plasmon polariton waveguides," Appl. Phys. Lett. **97,** 041107 (2010).
15. A. V. Krasavin and A. V. Zayats, "All-optical active components for dielectric-loaded plasmonic waveguides," Opt. Commun. **283,** 1581–1584 (2010).
16. N. C. R. Holme, P. S. Ramanujam, and S. Hvilsted, "10,000 optical write, read, and erase cycles in an azobenzene sidechain liquid-crystalline polyester," Opt. Lett. **21,** 902–904 (1996).
17. D. Y. Kim, S. K. Tripathy, L. Li, and J. Kumar, "Laser-induced holographic surface relief gratings on nonlinear optical polymer films," Appl. Phys. Lett. **66,** 1166–1168 (1995).
18. D. G. Zhang, X.-C. Yuan, A. Bouhelier, G. H. Yuan, P. Wang, and H. Ming, "Active control of surface plasmon polaritons by optical isomerization of an azobenzene polymer film," Appl. Phys. Lett. **95,** 101102 (2009).
19. K. G. Yager and C. J. Barrett, "Novel photo-switching using azobenzene functional materials," J. Photochem. Photobiol. A **182,** 250–261 (2006).
20. R. Loucif-Saibi, K. Nakatani, and J. A. Delaire, "Photoisomerization and second harmonic generation in disperse red one-doped and -functionalized poly(methy1 methacrylate) films," Chem. Mater. **5,** 229–236 (1993).
21. Z. Sekkat, D. Morichre, M. Dumont, R. Loucif-Saibi, and J. A. Delaire, "Photoisomerization of azobenzene derivatives in polymeric thin films," J. Appl. Phys **71,** 1543–1545 (1992).
22. F. S.-S. Chien, C. Y. Lin, and C. C. Hsu, "Local photo-assisted poling of azo copolymer films by scanning probe microscopy," J. Phys. D: Appl. Phys. **41,** 235502 (2008).
23. M. Dumont and Z. Sekatt "Dynamical study of photoinduced anisotropy and orientational relazation of azo dyes in polymeric films. Poling at room temperature," Proc. SPIE **1774,** 188–199 (1992).
24. I. K. Lednev, T.-Q. Ye, R. E. Hester, and J. N. Moore, "Femtosecond time-resolved uv-visible absorption spectroscopy of trans-azobenzene in solution," J. Phys. Chem. **100,** 13338–13341 (1996).
25. R. Rangel-Rojo, S. Yamada, H. Matsuda, and D. Yankelevich, "Large near-resonance third-order nonlinearity in an azobenzene-functionalized polymer film," Appl. Phys. Lett. **72,** 1021–1023 (1998).
26. C. B. Ma, D. Xu, Q. Ren, Z. H. Lv, H. L. Yang, F. Q. Meng, G. H. Zhang, S. Y. Guo, L. X. Sang, and Z. G. Wang, "Simple transmission technique for measuring the electro-optic coefficients of poled polymer films," J. Mater. Sci. Lett. **22,** 49–51 (2003).
27. J.-S. Bouillard, S. Vilain, W. Dickson, and A. V. Zayats, "Hyperspectral imaging with scanning near-field optical microscopy: applications in plasmonics," Opt. Express **18,** 16513–16519 (2010), `http://www.opticsinfobase.org/oe/abstract.cfm?URI=oe-18-16-16513`.
28. T. Holmgaard, S. I. Bozhevolnyi, L. Markey, A. Dereux, A. V. Krasavin, P. Bolger, and A. V. Zayats, "Efficient excitation of dielectric-loaded surface plasmon-polariton waveguide modes at telecommunication wavelengths," Phys. Rev. B **78,** 165431 (2008).

1. Introduction

Plasmonics has made a breakthrough in the field of integrated optics by overcoming the fundamental diffraction limit on the size of waveguide circuitry. The coupling of electromagnetic fields to free-electron oscillations at the metal/dielectric interface results in a surface wave - surface plasmon polariton (SPP), which can have larger wave vectors than that of light and thus a higher localization of photonic modes. Numerous geometries for SPP waveguides have been proposed [1], covering the whole range of localization levels and achievable propagation lengths all of which are finite due to Ohmic losses in metals. However, fully-functional integrated optical circuits require active plasmonic components capable of modulating and switching SPP signals. The nonlinear materials needed for implementation of all-optical functionality often have a trade-off between the achievable nonlinearities and the switching speed. Nevertheless, even the slow nonlinearities are useful in applications where small footprint components are needed to realize optically programmable and reconfigurable photonic circuitry.

Two important factors that govern the performance of an active component are the magnitude

#153017 - $15.00 USD Received 16 Aug 2011; revised 1 Nov 2011; accepted 11 Nov 2011; published 23 Nov 2011
(C) 2011 OSA

and speed of the induced transmission changes. The switching speed of a plasmonic modulator is largely dependent on the processes within an active material that are responsible for the index change of the active medium. It is always difficult to combine large modulation depth and fast switching speed due to the inherent properties of nonlinear optical materials, where in many cases the stronger nonlinearity the slower response time. Thermally driven processes are typically much slower than optical nonlinearity.

In the past, experimentally demonstrated plasmonic modulators have shown a range of switching speeds. Pacifici et al. [2] demonstrated an all optical modulator based on the interaction between SPPs in a thin absorptive layer of CdSe quantum dots (QDs) where the switching speed was $<$40 ns, in this case determined by fast intraband transitions in the CdSe quantum dots. Au nonolinearities in plasmonic nanorod metamaterial and Al nonlinearities in a flat film geometry provide sub-picosecond switching times [3, 4]. Pala et al. [5] show switching using photochromic molecules but the switching speed for useful modulation is slow ($\sim$10 s). Evans et al. [6] demonstrated an electro-optical cell consisting of gold nanorods covered with liquid crystals where the switching speed is relatively fast, depending on the liquid crystal polarization properties. Gosciniak et al. [7] demonstrate a thermo-optic plasmonic modulator with switching speeds in the order of seconds. However, this type of modulation was unique in terms of using a waveguide geometry which is not only efficient in terms localizing SPP propagation but also attractive for plasmonics based integrated technology.

In this article a compact resonant plasmonic element based on a waveguide ring resonator (WRR) having high sensitivity to the refractive index changes of the ring is used to demonstrate optically controlled signal transmission. This has been achieved doping a guiding polymer with disperse red 1 (DR1) molecules that provides large changes in the refractive index due to trans-cis isomerization. Such plasmonic components with low holding powers can be used in optically programmable and reconfigurable integrated photonic circuitry.

2. Results and discussion

Dielectric-loaded SPP waveguides (DLSPPWs, Fig. 1(a)), produced by a dielectric stripe placed on a metal surface, have proven to be an efficient means for guiding and manipulating plasmonic signals [8–12]. For a 500×440 nm^2 DLSPP waveguide at the telecommunication wavelength of $\lambda = 1550$ nm the plasmonic mode is localized at a subwavelength scale (Re(n_{eff}) $= 1.18$), while the propagation distance (at which the intensity decreases in e times) reaches 40 μm. Various DLSPPW-based photonic circuitry components have already been demonstrated including those with wavelength selective and resonant functionalities with a size on the order of a few micrometers [10]. For the realization of a plasmonic switching element, a plasmonic WRR geometry has been shown to be advantageous (Fig. 1(a)–1(c)) [12–14]. In this geometry, the transmission of the plasmonic signal is highly wavelength dependent due to the coupling of the incident signal to the resonant ring modes. In the first approximation, when the optical path around the ring is equal to an integer number of the mode wavelengths, the coupling is resonant, corresponding to a minima in the WRR spectral transmission characteristic. We implemented the ring resonator in a form of a racetrack (Fig. 1(b), 1(c)) and using finite element method (FEM) numerical simulations showed that by optimizing the WRR design (particularly curve radius R and center-to-center waveguide separation g), high modulation contrast with the wavelength can be achieved (Fig. 1(d)). If the refractive index of of the ring material n is changed by an external signal (either optical or electric), the effective index of the ring mode is modified and the resonance is shifted. Due to the high sensitivity of the WRR component, changes of $\Delta n \sim 10^{-3}$ are sufficient to change the mode transmission (Fig. 1(e)) and therefore an efficient active plasmonic component can be realized [7, 11, 15].

Azobenzene chromophores, such as DR1, are attractive materials for studying various sec-

#153017 - $15.00 USD Received 16 Aug 2011; revised 1 Nov 2011; accepted 11 Nov 2011; published 23 Nov 2011
(C) 2011 OSA

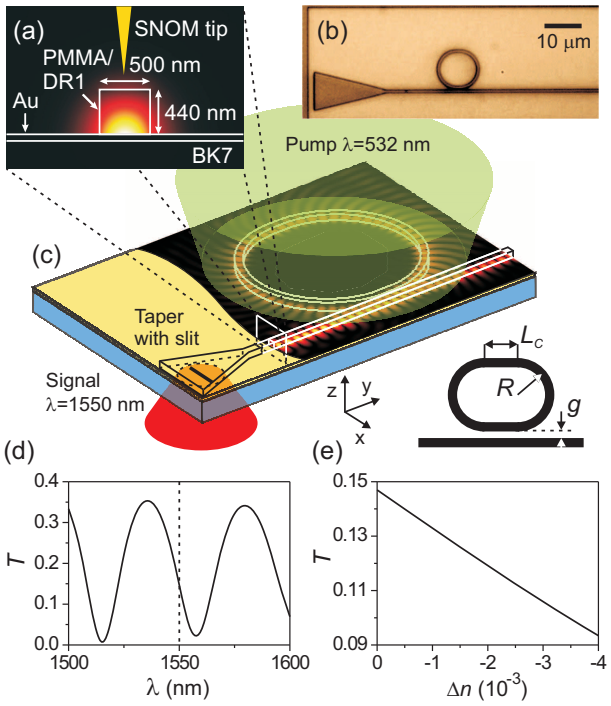

Fig. 1. (a) Cross-section of the 500×440 nm^2 WRR waveguide with the simulated P_y power flow profile of its fundamental TM_{00} SPP mode. (b) Optical image of the PMMA/DR1 ring resonator device. (c) Sketch of the experimental setup showing the signal and control light beams. Incorporated in the sketch is the simulated $|\mathrm{Re}(E_z)|$ cross-section of the SPP mode at the distance of 10 nm above the metal interface. (d) The wavelength dependence of the transmission T of the SPP mode through the WRR component simulated for the WRR with 500×440 nm^2 polymer waveguide, $R=4.971$ μm, $g=185$ nm), $L_c=1$ μm. (e) Dependence of the SPP mode transmission T on the refractive index of the ring simulated for $\lambda=1550$ nm (dashed line in (d)).

ond order nonlinear optical effects and polarized light-induced anisotropy. The photoinduced alignment of the azobenzene moieties on irradiation by linearly polarized light has been studied for several promising applications such as optical data storage and all-optical switching [16,17] and was proposed for changing the wave vector of SPP waves [18]. The structure of the pseudo-stilbene type azobenzene molecule consists of an azo group -N=N- between two benzene rings, and push-pull donor and acceptor groups on the opposite side of the benzene rings. Control light with a frequency near the main absorption resonance (490 nm) causes the azobenzene molecule to change from the trans to the cis configuration [19]. Since during this process the distance between the two carbon atoms is drastically reduced, the molecule's dipole moment as well as the materials polarizability is substantially changed, leading to dramatic changes in the materials refractive index. Due to the significant overlap between trans and cis absorption spectra [20], the pump light also initiates reverse isomerisation, happening simultaniously with thermal cis-trans relaxation [21]. These processes cause the molecules to oscillate between the trans and cis states under pump illumination [19, 22]. As the absorption probability for trans DR1 molecules is much higher for those predominantly oriented parallel to the pump polarisation, the isomerisation will deplete the population of such molecules, leading to light-induced anisotropy [22,23]. This mechanism is called angular hole burning and starts as soon as trans-cis-trans isomeri-

#153017 - $15.00 USD Received 16 Aug 2011; revised 1 Nov 2011; accepted 11 Nov 2011; published 23 Nov 2011
(C) 2011 OSA

sation is initiated. In addition, over longer pumping times, the trans-cis-trans isomerization cycling leads to statistical photo-orientation of the DR1 molecules perpendicular to the polarization of the pump light, which produces another, more slow, mechanism for light-induced anisotropy [19,22,23]. Azobenzene photoisomerization and light-induced birefringence occurs in the picosecond to second time range [20, 22, 24]. This depends on various factors, including the type of azobenzene moleciles, the environment surrounding them, the pumping wavelength and power. In the absence of radiation, the cis isomer thermally decays to the trans isomer. The birefringence relaxation ranges from minutes to milliseconds [20,21,23,25]. Illumination with unpolarised white light helps to restore a random distribution of DR1 molecules [18]. Overall, the light-induced birefringence on- and off- times depend on which of the two initiating mechanisms is dominant.

Nonlinear WRR components were fabricated in the following way. To obtain PMMA/DR1 composite material, DR1 and PMMA were separately dissolved in chlorobenzene. The DR1 solution was filtered (0.3 μm pore filter) to insure homogeneity and mixed with the PMMA solution to form 1 wt% DR1/PMMA ratio. These ratio were found to provide the strongest nonlinear response after testing materials of different compositions. A 440 nm thick PMMA/DR1 film was spin coated onto a 65 nm gold film and baked at 65° C for 4-5 hours in an oven and left overnight at room temperature to allow the solvent to evaporate. The components were patterned using electron beam lithography and then chemically developed to obtain WRR structure made from 500 nm wide DLSPP waveguides with a tapered coupling element (Fig. 1(b)). The ring resonator was implemented in a shape of a racetrack (two opposite semicircle sections connected by straight lines with length L_c, Fig. 1(c) rather then a ring in order to increase the interaction length between the ring and a straight waveguide. The use of racetracks allowed us to increase the distance between the racetrack and the straight waveguide whilst maintaining the same overall coupling efficiency (as for the circular ring), due to an increased interaction length. This increases the tolerances required from the fabrication process. Two sets of samples were studied with $L_c = 1$ μm (WRR A) and 2 μm (WRR B), having waveguide/ring edge-to-edge gap of 500 nm and ring radius R of 5 μm.

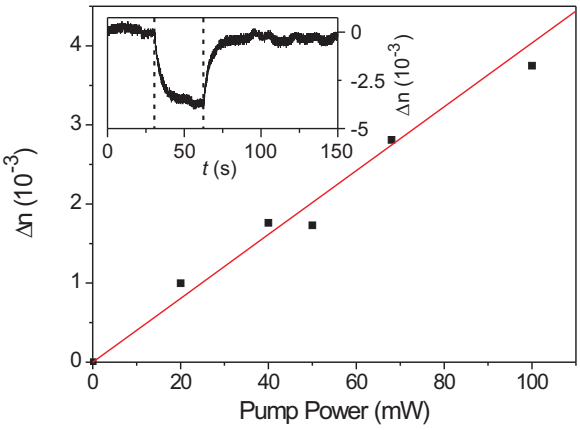

Fig. 2. The dependence of the refractive index change on the control light power. The 440 nm thick PMMA/DR1 film illuminated by the 532 nm control light. The inset shows the modulation dynamics for 110 mW control power, the duration of the control pulse is marked by the dashed lines.

#153017 - $15.00 USD Received 16 Aug 2011; revised 1 Nov 2011; accepted 11 Nov 2011; published 23 Nov 2011
(C) 2011 OSA

Optically-induced refractive index changes in the DR1/PMMA material were estimated in the pump-probe experiments on DR1/PMMA films deposed on a glass substrate (Fig. 2). Linearly polarized control light ($\lambda_c = 532$ nm) caused trans-cis isomerization of DR1 molecules accompanied by their reorientation perpendicular to the polarization direction, which changes the phase delay between the *p* and *s* components of the signal light ($\lambda_s = 633$ nm). The latter was monitored as a change in the signal transmission power with the sample placed between two crossed polarizers [26]. The resulting refractive index changes obtained from the dynamics at various pump powers is presented in Fig. 2. The observed on- and off- times are in agreement with previous observations [20–22]. Furthermore, the timescale of the processes and complete reversibility of the change suggests that the angular hole burning mechanism is responsible for the observed photoinduced birefringence. The optically induced refractive index changes increase linearly with the pump power with the absolute values reaching as much as $\Delta n = 3.7 \cdot 10^{-3}$ with no observable saturation. The refractive index changes are induced through optical nonlinearity and not thermally since pure PMMA films did not show refractive index changes at the light intensities used. Such large nonlinear changes in the refractive index will be more than sufficient for controlling the SPP mode transmission through the WRR component as modelled in Fig. 1(e).

The transmission of the SPP mode through fabricated racetrack WRRs was investigated using scanning near-field optical microscope (SNOM) operating in the tapping mode [27]. The 1550 nm light from a laser diode was mechanically modulated and focused on the slit in the tapered waveguide region using an ultrazoom objective system equipped with IR/visible camera (Fig. 1(c)). The slit fabricated using a focused ion beam is used in order to provide the SPP excitation in the waveguide. The near-field image of the SPP mode propagation was mapped by a metal-coated nano-apertured optical fibre. Signal from the fibre was detected by a photoreceiver and sent to a lock-in amplifier, having a signal from the chopper controller as a reference.

The near-field intensity distribution 0n WRR A along with the measured topography of the device are presented in Fig. 3(a), 3(b). The SPP wave generated by the slit propagates along the funnel, being adiabatically focused in the DLSPP waveguide. At the funnel region on the near field image there is a characteristic SPP interference pattern, which has been observed before in both numerical simulations and in near-field studies [28]. To the right of the funnel it was observed an SPP wave propagating at the gold/air interface; this corresponds to SPPs escaping the funnel. Further, a reflection of this wave from the ring can be observed. After focusing in the waveguide, the SPP mode propagates along it, being partially coupled to the ring mode in the region adjacent to the ring. It can be seen that the mode partially escapes from the racetrack on the curved parts, producing a characteristic SPP wave interference pattern in the area outside the ring. Please note that the intensity of the escaped light is greatly exaggerated ($\sim$5 times) in respect to the intensity of the mode, because it is directly collected by the SNOM tip, while the intensity of the DLSPPW mode is collected from the small evanescent field on the top of the waveguide (Fig. 1(a)).

To study an all-optical control of the SPP mode transmission, control light from a 532 nm laser diode was weakly focused (diameter $\sim$ 0.5 mm) onto the WRR region (Fig. 1(c)) and consequent SNOM images at various control powers were acquired. For each control power, the transmission was calculated as the ratio between the SPP intensities averaged over waveguide areas A_1 and A_2, before and after the ring region correspondingly (Fig. 3(b)). The resulting dependence of the WRR transmission on the control power is presented in Fig. 3(c) and is in agreement with the simulation results (Fig. 1(e)). The transmission decreases with the control light power since the initial transmission point is on the decreasing region of the WRR wavelength characteristic (as marked by a dashed line in Fig. 1(d)) and the resonance is blue-shifted due to the induced refractive index changes. Finally, we note that the decreasing nature of the

#153017 - $15.00 USD Received 16 Aug 2011; revised 1 Nov 2011; accepted 11 Nov 2011; published 23 Nov 2011
(C) 2011 OSA

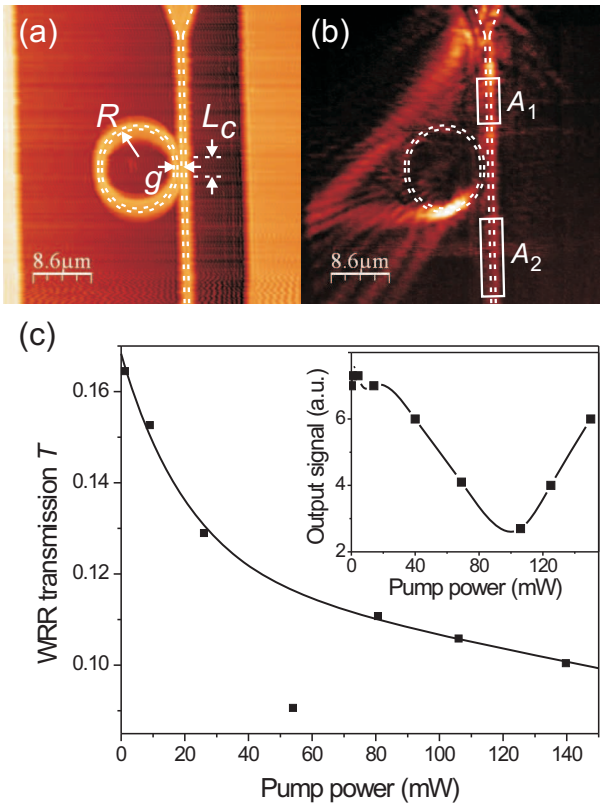

Fig. 3. (a) Topographic and (b) near-field images of the SPP mode intensity in the racetrack resonator. (c) The dependence of the SPP mode transmission through the WRR A on the control power derived from the averaging incoming and transmitted intensities from the near-field images as shown in (b). The line is to guide eye only. The inset shows the signal measured by monitoring the WRR transmission with the SNOM tip placed at the output of the WRR B.

WRR transmission rules out the possibility of an artefact created by the detection of control light coupled into the waveguide.

Even for low control powers of 20 mW a significant change in WRR transmission of more than 20 % is achieved, which can be attributed to two important factors. Firstly, the significant change in refractive index and secondly due to the very sensitive WRR transmission response to such changes. The relative transmission change is almost doubled up to $\sim$ 40 % as the control power approaches $\sim$ 100 mW. Although modulation performance of such a component is limited by the relaxation timescale ($\sim$ms), the dramatic optically-controlled change in the SPP mode transmission makes it a promising tool for active plasmonics circuitry to achieve optically reconfigurable components with low holding powers.

WRR B exhibits similar nonlinear behavior (Fig. 3(c) inset), but for its geometrical parameters the signal wavelength is closer to the transmission minimum and by changing the control power, it was possible to scan through the resonance. Both the method using with the measurements of the absolute WRR transmission (main panel in Fig. 3(c)) and the method monitoring the SPP output signal at the end of the waveguide (insert in Fig. 3(c)) produced complimentary

#153017 - $15.00 USD Received 16 Aug 2011; revised 1 Nov 2011; accepted 11 Nov 2011; published 23 Nov 2011
(C) 2011 OSA

results. Additionally we note, that the transmission changes are reversible: the device state with a low transmission (at $\sim$105 mW power in Fig. 3(c) inset) returns to the initial state with a high transmission after removal of the control light and several hours of white light illumination, suggesting the importance of molecular reorientation mechanism for the refractive index changes, initiated by several hours of the control light illumination during the SNOM measurements.

3. Conclusion

In conclusion, we have demonstrated a highly efficient nonlinear plasmonic component on the basis of a waveguide ring resonator device. The large nonlinear optical effects in PMMA/DR1 waveguide material based on trans-cis isomerization led to refractive index changes up to 4×10^{-3}. Combined with the highly resonant nature of WRR transmission, this resulted in reversible transmission changes of almost a factor of 3 times between high and low transmission states at milliwatt control powers ($\sim$100 W/cm^2 by intensity). Such components maybe used in optically reconfigurable and programmable plasmonic circuitry.

Acknowledgments

This work was supported by EPSRC (UK) and the Spanish Ministry of Sciences under grants FIS2010- 14834, CSD2007-046-NanoLight.es and Fundació privada CELLEX. The authors are grateful to Dr. Daniel O'Connor and Dr. Sebastien Vilain for their assistance in experiments. S.R. would like to thank Dr. Canek Fuentes-Hernandez and Prof. Bernard Kippelen at Georgia Institute of Technology for their guidance regarding the characterization of the isomerization of azobenzenes.

#153017 - $15.00 USD Received 16 Aug 2011; revised 1 Nov 2011; accepted 11 Nov 2011; published 23 Nov 2011
(C) 2011 OSA

194.207.135.200 {ts '2020-06-16 07:02:08'}